Anais do 57º Congresso Brasileiro do Concreto
CBC2015
Outubro / 2015

@ 2015 - IBRACON - ISSN 2175-8182

Pullout response of inclined fibres under direct shear

Segura-Castillo, Luis (1); Cavalaro, Sergio H. P. (2); Goodier, Chris I. (3); Austin, Simon A. (3); Aguado, Antonio (2)

(1) Universidad de la República. Montevideo, Uruguay.
Instituto de Estructuras y Transporte, Facultad de Ingeniería.
lsegura@fing.edu.uy
(2) Universitat Politècnica de Catalunya, UPC, Barcelona, Spain.
Department of Construction Engineering.
(3) Loughborough University, Loughborough, UK.
School of Civil and Building Engineering.

Abstract

Fibre-reinforced concrete (FRC) has been used as a structural material for many years, mainly in tunneling and industrial flooring. In recent years, new applications in which FRC can be partially or totally used in substitution of conventional steel reinforcement have appeared. Despite this, important issues regarding the behaviour and the design of FRC still have to be fully understood. For example, there is no direct analytical model universally accepted for design purposes to express and evaluate FRC behaviour under longitudinal shear. This paper therefore evaluates the response of single fibres under longitudinal shear to obtain information regarding the debonding and slipping behaviour of single fibres from the concrete matrix. Previous studies have been conducted with the fibres aligned with the load direction and perpendicular to the cracked plane. This arrangement however, is just one of an infinite number of possible arrangements that fibres could take up in any real application, where the fibres are likely to adopt a random distribution and orientation. Although models to predict the pullout response of fibres already exist (notwithstanding the inclination respect to the loading direction), these models were developed to model *tensile* behaviour. The objective of this study is therefore to propose a direct model to predict the pullout in *shear* of fibres embedded in a cementitious matrix. Therefore, one of the previous tensile models, is applied and extended to allow it to also describe the pullout behaviour of fibres under direct shear. This adapted model is compared with empirical data obtained from an existing experimental campaign on single fibres tested on direct shear. The results show a good agreement between the model and empirical data for displacements up to 10 mm, which represents an improvement in the capacity and accuracy of engineers to predict the behaviour of shear in FRC.

keywords: FRC, Pullout, shear, concrete, fibre

@ 2015 - IBRACON - ISSN 2175-8182

1. Introduction

Fibre-reinforced concrete (FRC) has been used as a structural material for many years, mainly in tunnelling and industrial flooring applications. However, new applications in which fibres have either partially or totally replaced the conventional reinforcement have appeared in recent years. An important milestone in the development of FRC was the publication of relevant design codes and recommendations that provided a scientifically founded, consistent and coherent framework for the design of FRC elements (Blanco et al. 2013). In most applications fibres are used to enhance the flexural tensile behaviour of the concrete. Nevertheless, fibres are also known to improve the shear behaviour, providing better performance to elements subjected to high and concentrated loads, or to seismic loads.

Although the fibre pullout in tension has been extensively studied (e.g. Robins et al. 2002), the same is not true for pullout in shear, possibly due to the experimental assessment of the shear response being difficult to perform to a satisfactory accuracy. This lack of existing published experimental studies reflects the absence of numerical models to predict the material's behaviour. Even though several models are proposed in the literature to assess the pullout response in *tension* (e.g. Laranjeira et al. 2009 and Laranjeira et al. 2010), to the authors' knowledge no direct analytical models to predict the pullout in shear has been published. This compromises the optimized design of elements subjected to longitudinal shear, and hence is a barrier to the fully efficient application of FRC.

The objective of this study is to therefore propose a direct model to predict the pullout in shear of fibres embedded in a cementitious matrix. The fibre pullout model herein described is based on conventional principles of mechanics. An analogy with the band line theory used in the design of prestressed tendons is made to estimate the response of the fibres. It takes into account the fibre-matrix bond and slip produced during the removal of a single fibre. It also considers the complex interaction between tangential and normal displacements during shear failure. The model is then validated using results obtained by Lee (2007), in which straight steel fibres with several inclinations were tested. The direct approach proposed here might serve as a reference for the design of elements of FRC subjected to shear in a safe and optimized way.

@ 2015 - IBRACON - ISSN 2175-8182

2. Single fibre pullout model in shear

2.1. Displacements

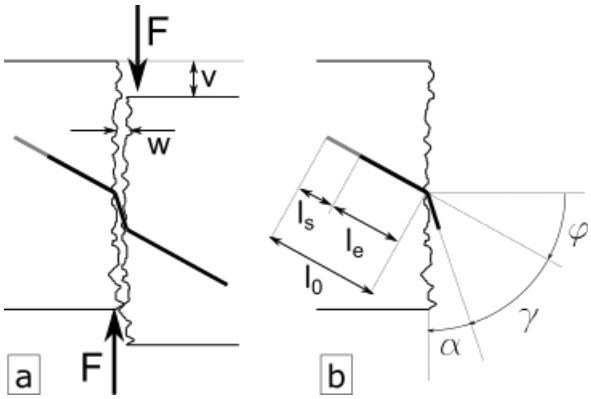

Fig. 1 – Possible displacements in the model: a) between two sides of the concrete; b) slip of embedded length of fibre, and bend of fibre outside concrete.

The proposed model represents the load vs. displacement relationships after a straight crack is formed, which splits the sample into two halves. The model is governed by the relative displacements that take place between the two halves. The crack is considered vertical, in line with the shear external forces applied (F) (Fig. 1a). It is also supposed that both sides of the concrete do not rotate. Therefore, there are two possible movements: opening of the crack (w) and slide of the crack (v) (Fig. 1a).

It is supposed that the fibre slips from only one side of the embedded parts, being l_0 the embedded length in the half that will slip (Fig. 1b). The *stretch* of fibre is considered negligible compared with the slip of the fibre. Therefore, the slip distance of the fibre can be calculated by *Eq. 1*

$$l_s = \sqrt{v^2 + w^2} \qquad \textit{Eq. 1}$$

where l_s is the slipped length of fibre at the moment of evaluation.

The part of the fibre still embedded can be calculated by *Eq. 2*

$$l_e = l_0 - l_s \qquad \textit{Eq. 2}$$

where l_e is the embedded length at the moment of evaluation.

The initial direction of the fibre is given by the angle φ, measured clockwise from the horizontal direction (Fig. 1b). Only positive angles are considered in this paper (the

@ 2015 - IBRACON - ISSN 2175-8182

evaluation of negative angles, which involve other more complicated phenomena, is currently in progress by the authors).

It is considered that bending of the fibre only take place at the exit points of the matrix. Therefore, in the exposed part of the fibre, between the two halves, the bending is negligible, and it is considered that the fibre goes straight from exit point to exit point in the two halves. The direction of the fibre (*α*) between exit points at both side of the crack can be calculated by *Eq. 3*

$$\tan(\alpha) = \frac{w}{v} \qquad \textit{Eq. 3}$$

Also, the angle of fibre bending (*γ*) at exit point can be calculated by *Eq. 4*

$$\gamma = 90^{o} - \alpha - \varphi \qquad \textit{Eq. 4}$$

2.2. Forces in the fibres

The load increase in the fibre is produced by interfacial shear stress (τ_f) provided by the fibre-matrix contact region (Fig. 2). Shear stresses can be provided by bond or by friction. In this model, it is considered that the bond is exhausted; therefore, only frictional stresses are considered. Two distinct zones are observed: a)- embedded straight length of fibre inside the matrix (Fig. 2a); b)- exit point of the fibre from the matrix (Fig. 2b).

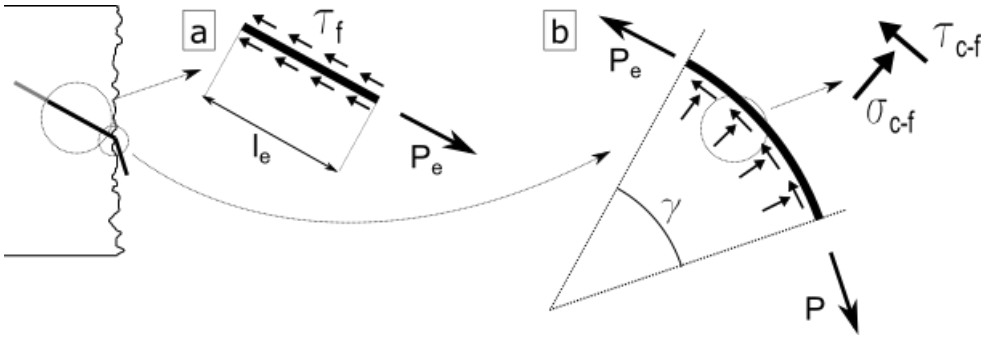

Fig. 2 – Development of forces in the fibre: a) embedded portion; b) exit-point

The load at the end of the straight part of the fibre embedded in the matrix can be calculated by *Eq. 5*

$$P_e = \int_{l_e} \tau_f(s).ds \qquad \textit{Eq. 5}$$

@ 2015 - IBRACON - ISSN 2175-8182

A simplification is used to solve *Eq. 5*. It is considered that τ_f is constant along the fibre, leading to *Eq. 6*

$$P_e = \tau_f^m * l_e \qquad \textit{Eq. 6}$$

Where τ_f^m is an average stress acting on the embedded length of the fibre.

Near the exit point of the matrix, the fibre has a concentrated bend. The bend produces an increase in the normal contact stress between fibre and matrix (See σ_{c-f} in Fig. 2b) which in turn increases the frictional response (see τ_{c-f} in Fig. 2b). Considering a linear relationship between normal and shear stresses due to friction (*Eq. 7*),

$$\tau_f = \mu_f * \sigma_f \qquad \textit{Eq. 7}$$

the load increase after the bend of the fibre can be calculated by the capstan equation (Bedford and Fowler 2008; Beer et al. 2013), already used to describe fibre behaviour by (Leung and Ybanez 1997; Soetens et al. 2013), as shown in *Eq. 8*

$$P = P_e * e^{\mu_f * \gamma} \qquad \textit{Eq. 8}$$

2.3. Forces through the cracked section

The global equilibrium of forces of one half of the concrete sample is shown in Fig. 3a. The vertical external load (F) is balanced by forces produced by the fibre bridging the crack, and by friction forces produced by the concrete-to-concrete interaction.

The fibre load can be decomposed into two forces acting in the crack direction and in the respective orthogonal direction (See Fig. 3c), according to *Eq. 9*

$$P_V = P * \cos(\alpha) \qquad \& \qquad P_H = P * \sin(\alpha) \qquad \textit{Eq. 9}$$

The fibre bridges both parts of the split concrete, therefore, a normal concrete-to-concrete stress (σ_c) is considered acting through the surface of the cracked section. Associated with this normal force there may be a concrete-to-concrete shear force (τ_c), as is shown in Fig. 3b.

@ 2015 - IBRACON - ISSN 2175-8182

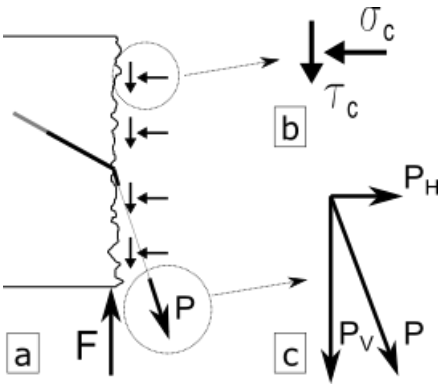

Fig. 3 – Forces through the cracked section: a) general scheme; b) concrete-to-concrete friction; and c) fibre load.

In the moment where the two halves of concrete slip, the relationship between shear and normal stress can be expressed by a friction equation (*Eq. 10*)

$$\tau_c = \mu_c * \sigma_c \qquad \textit{Eq. 10}$$

Where μ_c is the concrete-to-concrete friction coefficient.

2.4. Equilibrium of forces

As it is supposed that both sections at each side of the crack do not rotate, the equilibrium is satisfied just if the sum of forces is zero. Expressing this sum in the two main orthogonal directions leads to *Eq. 11* and *Eq. 12*

$$\sum F_H = 0 \therefore P_H = \int_{A_c} \sigma_c dA \qquad \textit{Eq. 11}$$

$$\sum F_V = 0 \therefore F = P_V + \int_{A_c} \tau_c dA \qquad \textit{Eq. 12}$$

2.5. Solving the system

Replacing *Eq. 10* and *Eq. 11* in *Eq. 12* leads to *Eq. 13*.

$$F = P_V + \int_{A_c} \mu_c * \sigma_c dA = P_V + \mu_c \int_{A_c} \sigma_c dA \Rightarrow F = P_V + \mu_c * P_H \qquad \textit{Eq. 13}$$

Replacing *Eq. 9* in *Eq. 13* leads to *Eq. 14*.

@ 2015 - IBRACON - ISSN 2175-8182

$$F = P_V + \mu_c * P_H = P * \cos(\alpha) + \mu_c * P * \sin(\alpha) = P * (\cos(\alpha) + \mu_c * \sin(\alpha)) \qquad \textit{Eq. 14}$$

Finally, replacing *Eq. 8* in *Eq. 14* leads to *Eq. 15*.

$$F = P_e * e^{\mu_f * \gamma} * (\cos(\alpha) + \mu_c * \sin(\alpha)) \qquad \textit{Eq. 15}$$

Using the equations presented in this section the total force provided by the matrix-fibre system can be determined based upon the embedded fibre length (l_0), the mechanical characteristics (τ_f^i, μ_f, μ_c) and the relative displacements between the two concrete halves (v, w).

3. Displacements

As seen in the previous section, the model is based upon the relative displacements at both sides of the crack. Therefore, the experimental results of samples tested under shear (Lee, 2007) could be analyzed and a simplified numerical displacement law deduced in order to consider the displacements in the shear model.

Fig. 4 represents the displacements of individual fibres during the shear tests. Fig. 4a shows the experimental results in continuous lines, overlapped with the numerical simplification shown in dotted lines. Notice that the vertical displacements are larger than the horizontal, hence the use of different scales for the axes. A good agreement between the experimental results and the simplified law can be observed, as described below.

For the simplified law it is considered that the displacements are divided into three main zones: an initial dilatancy, the slide, and the pullout.

The initial dilatancy (the increase in the horizontal displacement when the vertical slide increases) varies in intensity and length depending upon the orientation of the fibre. Fig. 4b shows the representation of the displacements in an “isotropic” scale (i.e. the same scale for the horizontal and vertical direction). It can be seen that in the beginning of the displacements, the direction of the fibre governs the direction of the displacement, i.e. the initial orientation of the fibre determines the direction of the initial crack opening. This seems reasonable if it is considered that the fibre produces a dowel action between the two halves of concrete. Also, it is observed that the length of this stage is larger as the angle increases.

@ 2015 - IBRACON - ISSN 2175-8182

In the second stage, the fibres slide with a relatively constant increase in the dilatancy. The length of this stage is larger for smaller angles. Finally, there is a more or less horizontal displacement previous to the final pullout of the fibre.

For the simplified law only the first two stages were considered. The slope of the first stage corresponds to the orientation of the fibre. For the second stage, the same slope was considered for all the orientations. Therefore, only this slope and the initial and final point of the second stage had to be estimated to obtain the complete laws to describe the displacements.

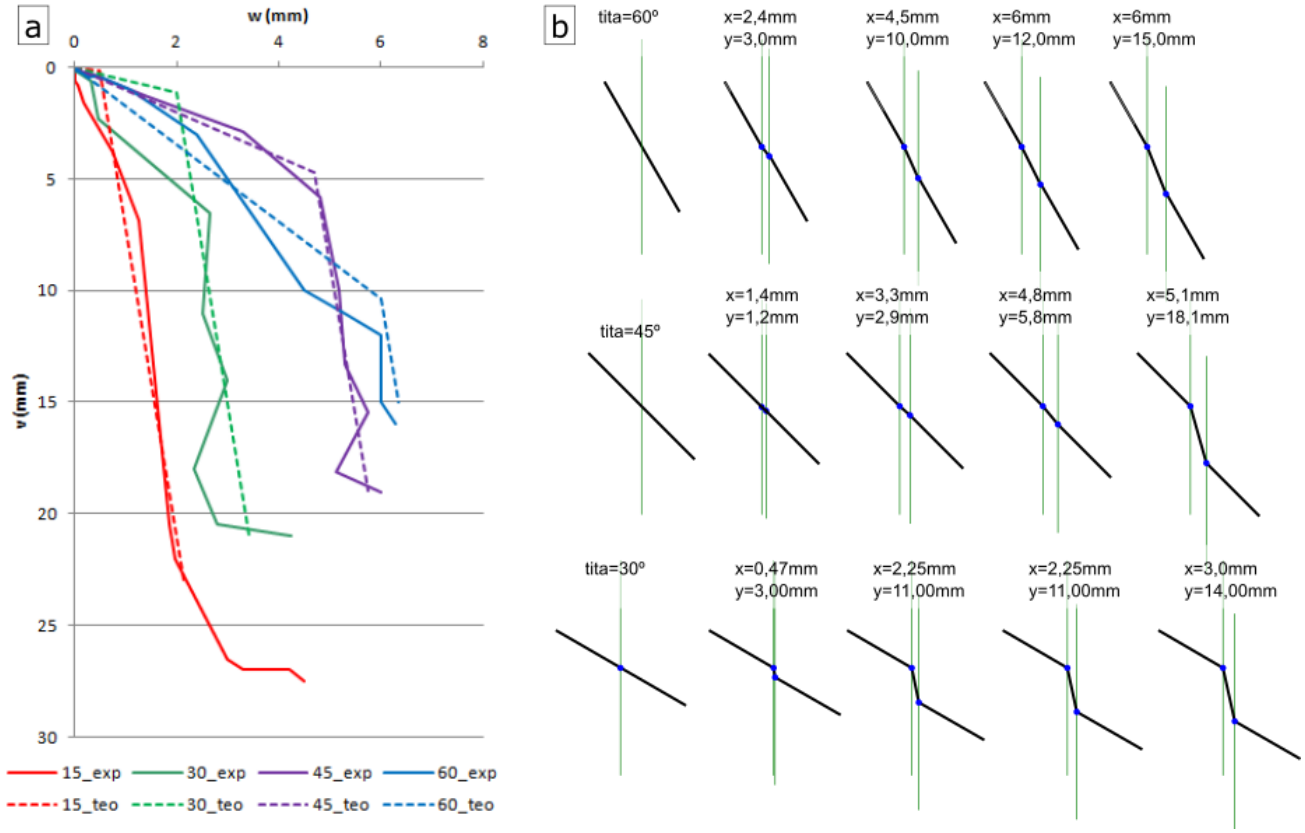

Fig. 4 – Single fibre displacements: a) vertical vs. horizontal displacements for each orientation; b) representation of displacements for some directions with same horizontal and vertical scale.

4. Results

The model was calibrated with experimental results taken from Lee (2007). The concrete-to-concrete friction coefficient was also taken from literature (μ_c=0,75). A “trial and error” procedure was used to obtain the other parameters.

@ 2015 - IBRACON - ISSN 2175-8182

Fig. 5 shows the load vs. displacement results for the model (in colour lines) overlapped with the experimental results (grey and black lines). For the model curves, each line represents an inclination angle of the fibre.

A good agreement in the first 5 to 10 mm of displacements can be observed. The accuracy then gradually decreases from 10 mm towards the end of the plot. It can be seen that the model is incapable of representing the relatively constant load values that the experimental results show for displacements between 10 and 20 mm for all the inclination angles.

For engineering applications the behaviour of the first few millimetres of displacement are most important, as it is considered that the concrete would be under failure with larger crack displacements. However, it would still be important to reproduce the entire curve to validate the model.

A notable difference between the experimental and numerical results is the final displacements in the moment of extraction of the fibre. The experimental results show different displacements for the different angles, an aspect that this model has not been able to reproduce.

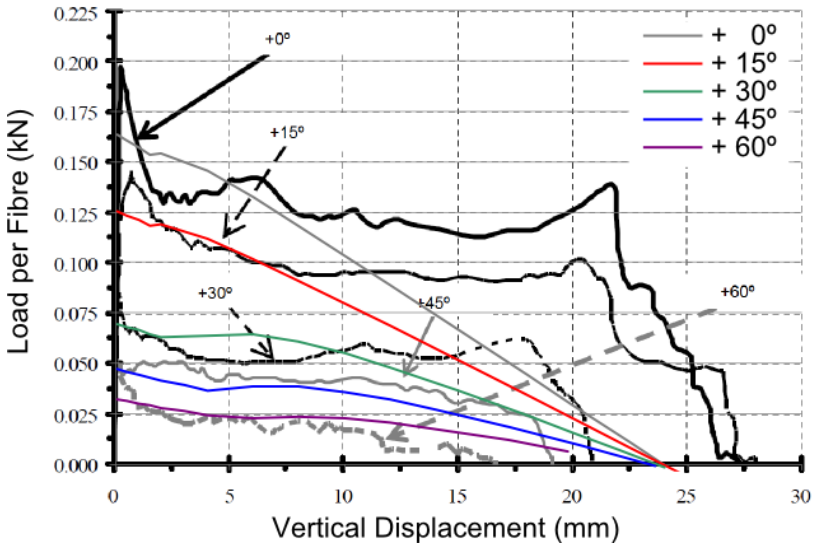

Fig. 5 – Load versus displacement plot for model and experimental results

The previous results are broken down in Fig. 6, showing the contribution of the three main terms of *Eq. 15* to the total load.

The variation of the first term (P_e) is shown in Fig. 6a. An almost linear variation can be observed, from the maximum load when the fibre is fully embedded, decreasing as the

@ 2015 - IBRACON - ISSN 2175-8182

fibre is pulled out of the matrix. The dilatation (horizontal displacement) produces the small registered non-linearity. Although it is reasonable that the load decreased from its maximum value when the fibre is fully embedded to a null value previous to its pull off from the matrix, it is possible that the curve described is not close to a linear variation. For the author's opinion, the linearity assumption with the embedment length is the main cause that leads to the difference in the model for displacements larger than 10 mm, and further analysis should be conducted.

The variation of the second term ($e^{\mu_f * \gamma}$) is shown in Fig. 6b. This term reproduces the increase in the pullout load produced by the concentrated bend at the fibre exit point of the matrix. This term modifies to a large extent the value of P_e, from values around 1,0 (for the fibres in +60º) to values of almost 4,5 (for fibres in +0º). Therefore, according to the model, the large differences registered in the loads for the different angles are provided by this effect.

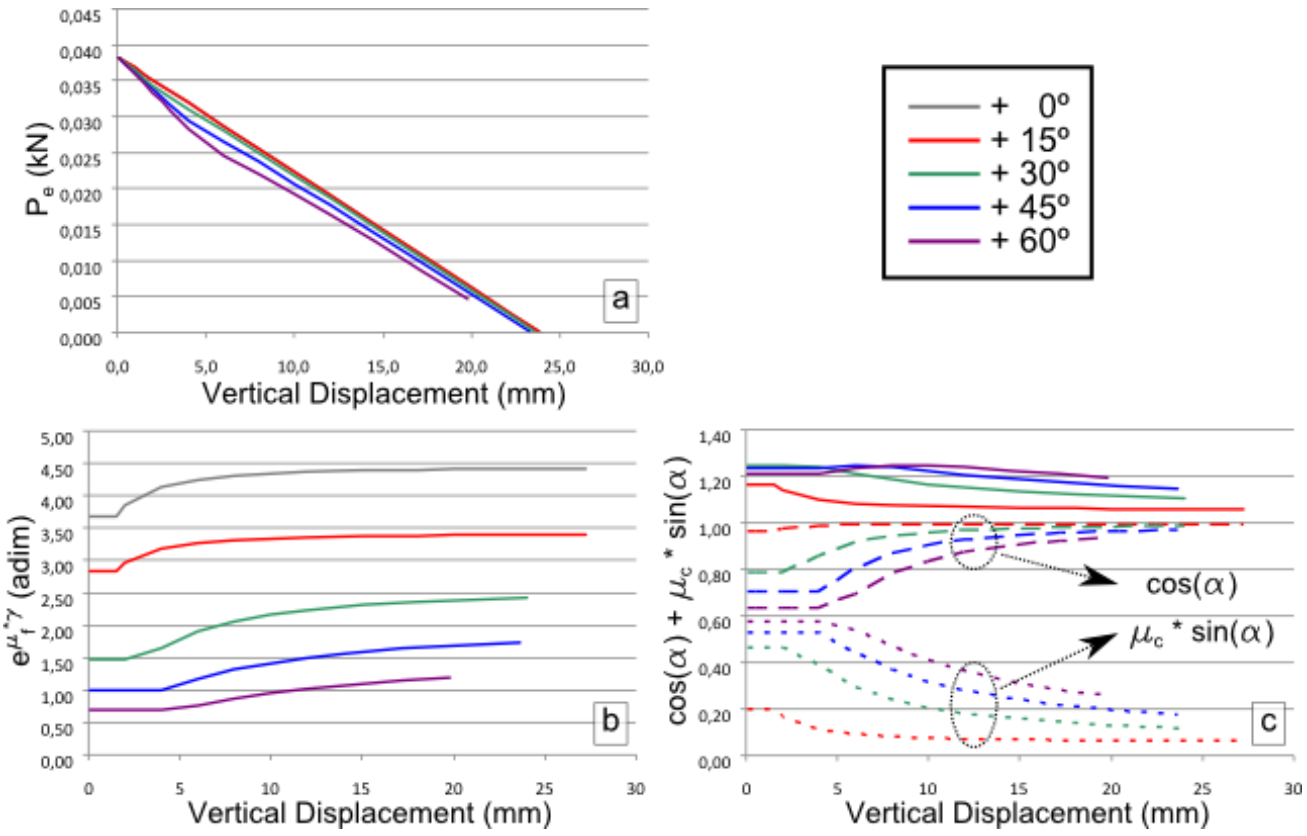

Fig. 6 – Decomposition of the model results in the three main terms of Eq. 15: a) P_e; b) $e^{\mu_f * \gamma}$; c) $\cos(\alpha) + \mu_c * \sin(\alpha)$.

@ 2015 - IBRACON - ISSN 2175-8182

Finally, the variation of the third term, "$(\cos(\alpha)+\mu_c*\sin(\alpha)$", is shown in Fig. 6c. The plot also shows each of the components of the addition: "$\cos(\alpha)$"; in dashed lines, and "$\mu_c*\sin(\alpha)$"; in dotted lines.

The influence of the bridging direction components (angle *α*) is greater at the beginning of the displacements, tending to the stabilization as the concrete slips. The dilatation takes place mainly at the beginning of the displacements, then, as the vertical displacement increases, the angle α tend to zero, and therefore, the entire term to 1. The total influence of this term is much smaller than the second term, reaching a maximum increase smaller than 1,3.

5. Conclusions

A direct model to predict the load-displacement response of the pullout of fibres under longitudinal shear is presented. The model is based upon mechanical characteristics, and in the relative displacement experienced in the cracking plane. The analyses performed confirm the capacity of the model proposed to reproduce the experimental load-displacement curves obtained by Lee (2007).

The results show good agreement for displacements up to 10 mm. For larger displacements, the model predicts a constant reduction in the shear force resisted, whereas the experimental results indicate an almost constant load. This may be attributed to possible inaccuracies regarding the assumption of a constant friction in the embedded part of the fibre. Despite this, the good fit obtained in the initial part of the load-displacement curve represents an improvement in the capacity of engineers to predict the behaviour of FRC in shear, as higher levels of displacement rarely occur in practice.

Acknowledgments

The authors want to thank the Spanish Ministry of Science and Innovation for the economic support received through Research Project IPT F-00339 FIBHAC.

@ 2015 - IBRACON - ISSN 2175-8182

6. References

Bedford, A. and Fowler, W., 2008. *Engineering Mechanics: Statics (5th ed.)*, NJ: Pearson, Upper Saddle River, USA.

Beer, F.P. et al., 2013. *Vector Mechanics for Engineers: Statics and Dynamics, (10th ed.)*, New York: McGraw-Hill, USA.

Blanco, A., Pujadas, P., de la Fuente, A., Cavalaro, S., Aguado, A., 2013. Application of constitutive models in European codes to RC–FRC. *Construction and Building Materials*, 40, pp.246–259. Available at: http://linkinghub.elsevier.com/retrieve/pii/S095006181200774X [Accessed July 17, 2013].

Laranjeira, F., Aguado, a. and Molins, C., 2009. Predicting the pullout response of inclined straight steel fibers. *Materials and Structures*, 43(6), pp.875–895. Available at: http://www.springerlink.com/index/10.1617/s11527-009-9553-4 [Accessed November 9, 2014].

Laranjeira, F., Molins, C. and Aguado, a., 2010. Predicting the pullout response of inclined hooked steel fibers. *Cement and Concrete Research*, 40(10), pp.1471–1487. Available at: http://linkinghub.elsevier.com/retrieve/pii/S0008884610001249 [Accessed February 16, 2014].

Lee, G.G., 2007. *Direct Shear Behaviour of Steel Fibres in a Cementitious Matrix*. PhD Thesis. The University of New South Wales, Australia. Available at: http://www.unsworks.unsw.edu.au/primo_library/libweb/action/display.do?tabs=detailsTab&ct=display&fn=search&doc=unsworks_1610&indx=7&recIds=unsworks_1610&recIdxs=6&elementId=6&renderMode=poppedOut&displayMode=full&frbrVersion=&dscnt=1&scp.scps=scope%3A(LRS_UNSWORKS)&frbg=&tab=default_tab&dstmp=1338291445406&srt=rank&mode=Basic&dum=true&tb=t&vl(freeText0)=lee&vid=UNSWORKS [Accessed May 29, 2012].

Leung, C.K.Y. and Ybanez, N., 1997. Pullout of inclined flexible fiber in cementitious composite. *Journal of Engineering Mechanics*, 123(3), pp.239–246.

Robins, P., Austin, S. and Jones, P.A., 2002. Pull-out behaviour of hooked steel fibres. *Materials and structures*, 35(August), pp.434–442. Available at: http://www.springerlink.com/index/LT666G846100N566.pdf [Accessed April 24, 2012].

Soetens, T., Van Gysel, A., Matthys, S., Taerwe, L., 2013. A semi-analytical model to predict the pull-out behaviour of inclined hooked-end steel fibres. *Construction and Building Materials*, 43, pp.253–265. Available at: http://dx.doi.org/10.1016/j.conbuildmat.2013.01.034.